Original scientific paper

Formation and reduction of anodic film on polycrystalline Bi electrode in pure methanol solutions

Anastos G. Anastopoulos$^{\boxtimes}$ and Athanasios A. Papaderakis

Laboratory of Physical Chemistry, Department of Chemistry Aristotle University of Thessaloniki, 54124 Thessaloniki, Greece

Corresponding author: $^{\boxtimes}$anasto@chem.auth.gr

Abstract

The processes of film formation and reduction of bismuth in pure methanol are phenomenologically studied by means of cyclic voltammetry, ac voltammetry and electrochemical impedance spectroscopy methods. Film formation takes place under low electrode potentials within the potential range from -0.1 to about 0.2 V vs. Ag|AgCl resulting in the development of $Bi(CH_3O)_{ads}$ layer. The scan rate effect on the anodic current profile is interpreted in terms of a gradual variation of uncompensated resistance, accompanying the processes of film formation and reduction. Phase sensitive ac voltammetry measurements suggest leaky insulating character of a thin anodic film in agreement with the results of electrochemical impedance experiments.

Keywords
Anodic film formation; bismuth; methanol, methoxylation

Introduction

Electrochemical studies have confirmed that in pure methanol solutions methoxy anions, resulting from the solvent self-dissociation, interact with various electrode materials *viz*. Cu, Ni, Zn, Fe Ti, Si and the valve metal Al. This interaction leads to the formation of anodic surface films of the general type $M-(CH_3O)_n$, where M is the electrode material and n depends on the dissolution reaction of the electrode material and the specific reaction of film formation [1-3]. It is surprising that up to now, there is nothing reported in the literature about the electrochemical study of another valve metal Bi in pure methanol solutions. On the contrary, long-lasting systematic electrochemical research has been devoted to the system Bi/H_2O. In aqueous solutions, Bi_2O_3 is anodically formed on Bi surface by diffusion and field assisted migration of Bi^{3+} ions through the film under the influence of the so-called high field mechanism [4], resulting in both thickening and spreading of oxide islets. The cathodic reduction of Bi_2O_3 [5] involves development of a metallic Bi

film at the oxide/electrolyte interface, which is extended towards the interior of Bi_2O_3 layer. Two possible reduction mechanisms are usually suggested, the first involving electron transfer in the film and reduction at the film/solution interface and the second one, involving ion transfer in the film and reduction at the metal/film interface [6]. Bi_2O_3 oxide can be completely reduced by electrochemical means. Bi_2O_3 anodic oxide films present electrical rectification by acting as insulators under anodic potentials and conductors under cathodic ones, respectively [7,8]. Another important feature of Bi_2O_3 layers is their photoconductivity in the visible region. Bi_2O_3 layers present photocurrents of n- and p-type, thus being characterized as amphoteric semiconductors. The query as to whether Bi/CH_3OH system possesses similar or different properties than Bi/H_2O has motivated us to get involved in the present work.

Experimental

Electrodes and Chemicals

A polycrystalline Bi rod (Alfa Aesar, 99.99 %) embedded in a glass cylinder, sealed by suitable adhesive and covered with thermoplastic tube to leave a free disk shaped surface of 8 mm diameter at its end, was used as a working electrode. Pt foil auxiliary electrode and Ag|AgCl reference electrode saturated with aqueous KCl, both placed in a single compartment of double walled electrochemical cell kept at 298 K, were used in all measurements.

0.1 M $LiClO_4$ in methanol is used as the base solution in all measurements.

The working electrode was mechanically polished by emery paper of decreasing grain size. After that it was set for several minutes in an ultrasonic bath containing distilled water. Then it was washed with the working solution and transferred rapidly to the electrochemical cell.

The chemical reagents used without further purification are anhydrous $LiClO_4$ (Aldrich 99.99 %) and methanol (Lab-Scan, purity >99 %, maximum water content 0.05 %).

Methods and Instrumentation

Cyclic voltammetry and electrochemical impedance spectroscopy (EIS) measurements were carried out by Autolab PGSTAT302N electrochemical system connected to a PC running the Autolab software.

Bi electrode activation was proved necessary to improve the reproducibility of all electrochemical measurements. Therefore, Bi electrode was activated by cyclic voltammetry, scanning the potential from -1.6 to 0.2 V and back to -1.6 V *vs.* Ag|AgCl with a rate of 0.025 V s^{-1}. EIS measurements were carried out within the frequency range of 10 kHz to 0.1 Hz with 4 mV *ac* signal amplitude at selected *dc* potentials. The reproducibility of all electrochemical impedance measurements was checked by the comparison of three successive measurements at the same potential. The linearity-stability conditions for EIS measurements were checked by the Kramers-Kronig test incorporated in the AUTOLAB software. By this procedure, the sum of squares of differences (chi-square) between measured and calculated complex impedance values, *i.e.* real and imaginary impedance values were found to be of the order of 10^{-2} in all systems studied within the frequency range from 10 kHz to 0.5 Hz. At frequencies below 0.5 Hz some EIS measurements were omitted because the corresponding chi-square values were found not better than 10^{-1}. Phase selective ac voltammetric measurements were carried out by an experimental setup [9] comprising a lock-in amplifier (model SR830 from Stanford Research) and a potentiostat (model Potentioscan Wenking POS73 from Bank Elektronik), interfaced to a PC running LabVIEW 6.1. Negative *dc* potential scan was applied in steps of 25 mV from 0.20 to -1.60 V *vs.* Ag|AgCl. Each measurement was taken after 10 s of stopover at

each potential. The amplitude and the frequency of the *ac* signal were set to 4 mV and 80 Hz respectively. The standard deviation between at least three successive measurements, expressed on a percent basis, was found equal to about 5 %.

Results and discussion

Cyclic voltammetry

The cyclic voltammetry response of a polycrystalline Bi electrode in pure methanol solution of 0.1M LiClO$_4$, obtained with an electrode potential scan rate ranging from 0.025 to 0.4 V/s is shown in Figure 1.
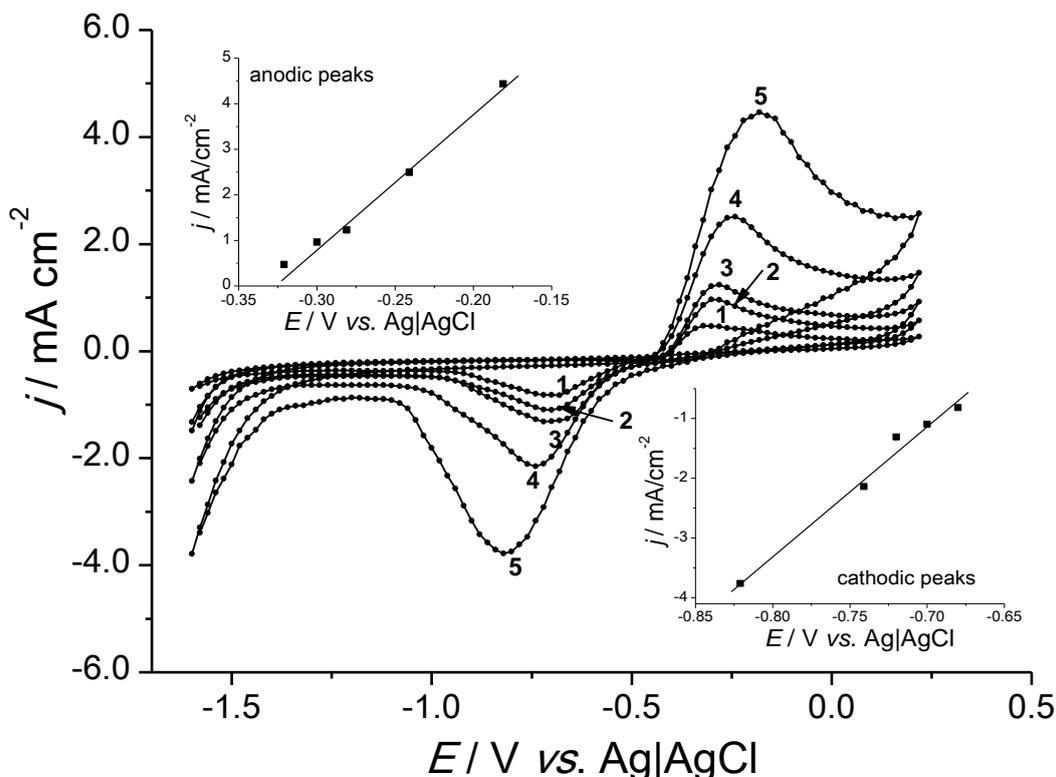
Figure 1. *Cyclic voltammetry curves of Bi in methanol solution of 0.1 M LiClO$_4$ at various scan rates: (1) 0.025, (2) 0.05, (3) 0.10, (4) 0.20, (5) 0.40 V/s. Insets: Anodic and cathodic peak currents vs. corresponding peak current potentials.*

During the anodic scan, the characteristic features of voltammetry curves are the following: At potentials positive to -0.40 V *vs.* Ag|AgCl, the anodic current increases leading to a single anodic current peak, which depending on the scan rate is located within the potential range (-0.25±0.07) V *vs.* Ag|AgCl. This peak marks the formation of initial nuclei of the anodic film. The absence of multiple anodic peaks indicates that successive layers are not developed. At potentials positive to the anodic peaks, the current *vs.* potential dependence presents a narrow and ill-defined plateau which tends to a new increase of anodic current at electrode potentials, $E \geq 0.20$ V *vs.* Ag|AgCl. This current increase is presumed to be related to the methanol oxidation on Bi, the exact mechanism of which is neither known nor the subject of the present work. However, it can be reasonably assumed that $E \approx 0.20$ V *vs.* Ag|AgCl is the positive limit of anodic film formation in the neutral methanol solution of 0.1 M LiClO$_4$. During the cathodic scan, the characteristic features of voltammetric curves are the following: The single cathodic current peak observed at

(-0.75±0.07) V *vs.* Ag|AgCl is presumed to be related to the reduction process of the anodically developed film. At potentials negative to -1.40 V *vs.* Ag|AgCl, however, the hydrogen evolution manifests itself by increase of the cathodic current.

The observed single anodic and cathodic peaks suggest that formation and reduction processes of the anodic film in the case of the system Bi/CH$_3$OH represent one step reactions. At potentials from about -0.1 V to 0.2 V *vs.* Ag|AgCl, where ill-defined anodic plateau of the curves of Figure 1 is observed, anodic films of Bi in methanol are developed. Although the decomposition of methanol is a rather complicated process resulting in various ionic species of the general type CH$_x$O [1], the process of its self-dissociation can be simply described as:

$$2CH_3OH \leftrightarrow CH_3O^- + CH_3OH_2^+ \tag{1}$$

Combination with the simple picture of voltammetric curves of Figure 1, suggests that the process of anodic film formation of bismuth in pure methanol is presumably its surface methoxylation. At low positive and negative electrode potentials CH$_3$O$^-$ ions are electrosorbed on the Bi surface, which undergoes a single step anodic dissolution, as deduced by the single anodic peak. Formation of Bi$^+$ is, similarly to that suggested for Al [1], carried out according to the reaction:

$$Bi \rightarrow Bi^+ + e \tag{2}$$

Presumably, a thin film of the form Bi(CH$_3$O)$_{ads}$ is developed on the bare metal Bi. Single anodic peaks also suggest that Bi$^+$ is the final dissolution product and that further dissolution of bismuth is not detected in pure methanol. Therefore, the anodic film formation of Bi in pure methanol can be described by means of the following one-electron reaction [1]:

$$Bi^+ + CH_3O^- \rightarrow Bi(CH_3O)_{ads} + e^- \tag{3}$$

Correspondingly, during the cathodic scan, the reduction of Bi(CH$_3$O)$_{ads}$ film is reasonably expected to take place by means of the inverse reaction (3).

According to the literature [10-13], a mechanistic interpretation of the nucleation and thickening of anodic films can be formulated by means of the relation between the anodic current profile and the electrode potential scan rate. In Figure 1 we see that with increasing the scan rate, peak currents increase, and anodic peaks shift to more positive potentials, while cathodic peaks shift to more negative ones. Peak potential and peak current values are linearly dependent on the square root of the scan rate as indirectly indicated by linear *j* peak *vs. E* peak plots shown in the insets of Figure 1. Such linear dependencies involving peak currents and peak potentials were already reported [14] for Bi$_2$O$_3$ anodic film developed on Bi surface in aqueous solutions. The formation and reduction mechanisms of Bi$_2$O$_3$ include the occurrence of a solid state diffusion process [13,14] operating only in the case of thick films developed under high positive electrode potentials. This would not be the case for the thin anodic layer Bi(CH$_3$O)$_{ads}$ formed in pure methanol. In this case the linear dependence of *E* peak and *j* peak values on the square root of scan rate may be the result of a gradual variation of uncompensated resistance, accompanying the film formation and reduction according to the so called passivation model of Müller, where the process of film formation is under the control of ohmic resistance [10].

Phase selective ac voltammetry

Information about the structural characteristics of an electrochemical interface can be also acquired from differential capacitance measurements.

However, over the whole potential range studied from 0.2 to -1.6 V *vs.* Ag|AgCl, the interface between the polycrystalline Bi electrode and methanol solution may be not identified with the

model of ideal capacitor, because at the extremes of this range Bi/methanol interface is not ideally polarizable. It must also be indicatively recalled that capacitance studies of single crystal Bi electrodes in $LiClO_4$ containing methanol solution performed by Estonian electrochemists [15], were carried out at electrode potentials ranging from -0.4 to -1.4 V *vs.* SCE leaving outside the potentials where film formation and hydrogen evolution occur. In this respect, it is useful to look at the structural characteristics of Bi/CH_3OH interface by means of the phase selective *ac* voltammetry technique in terms of the potential dependence of the out of phase *ac* current, j_{90}, decoupled from the in phase j_0 component. j_{90} *vs. E* curves are typically free from faradaic contributions and describe the potential dependence of the resident interfacial charge, providing thus a picture of the structural condition of the interface. In Figure 2, j_{90} *vs. E* dependence clearly shows potential regions where the anodic film is present and those where it is absent.
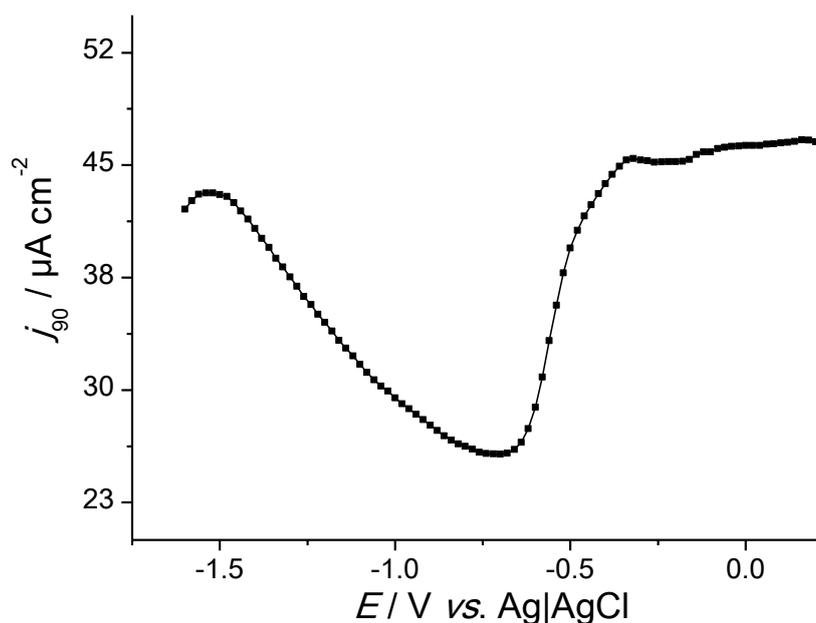
Figure 2. *Electrode potential,* E*, dependence of out of phase current,* j*₉₀, at polycrystalline Bi electrode in 0.1 M LiClO₄ methanolic solution.*

At potentials positive to -0.50 V *vs.* Ag|AgCl where the anodic film is present, j_{90} values show a weak potential dependence. According to the literature [16], potential independent capacitance may be expected for insulating films having thicknesses of about $(1.5\pm0.5)\times10^{-7}$cm. Thus, the weak potential dependence of j_{90} current values shown in Figure 2 may be considered as an indication for the presence of a leaky insulating film prior than passive or semiconductive layer of oxide nature.

The minimum of j_{90} *vs. E* curve in Figure 2 falls into the same potential range as cathodic peaks of cyclic voltammetric curves shown in Figure 1. Therefore, it may be assumed that the potential dependence of j_{90} from about -0.50 V to -0.85 V *vs.* Ag|AgCl represents a transition from the $Bi(CH_3O)_{ads}$ covered electrode to the bare metal Bi.

Electrochemical impedance spectroscopy

The elucidation of processes involved in the formation and reduction of $Bi(CH_3O)_{ads}$ surface film can be further assisted by electrochemical impedance measurements, carried out at selected electrode potentials. As shown in Figure 3, all Nyquist plots obtained at the vicinity of the anodic and cathodic peaks *i.e.* at -0.4 V and -0.68 V and also at -1.4 V *vs.* Ag|AgCl where hydrogen evolution is presumed, exhibit the form of flattened semicircles.

-Z'' vs. Z' plots of Figure 3 can be approximated by the Randles circuit of the type $R_s(R_{ct}Q_{dl})$ according to the circuit description code of Boukamp [17]. This circuit incorporates solution and charge transfer resistances (R_s and R_{ct}) and the parameter Q_{dl} of the constant phase element which resembles the contribution of double layer capacitance to the overall impedance.
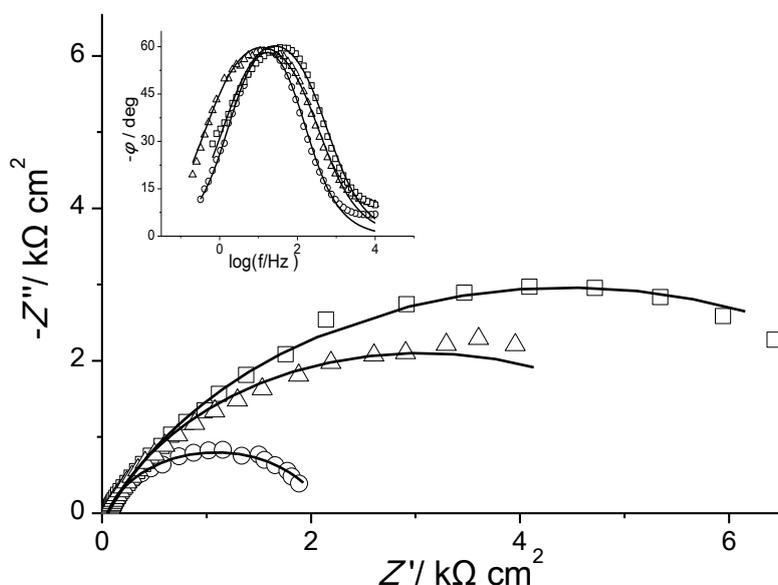
Figure 3. *Nyquist plots of Bi in methanol solution of 0.1 M LiClO$_4$, at various electrode potentials in V vs. Ag|AgCl: △ -0.4, □ -0.68, ○ -1.4. Inset: Bode phase diagrams at the same potentials. Lines represent simulated responses fitted to experimental points.*

The corresponding Bode phase diagrams shown in the inset of Figure 3 clearly show a single *RC* time constant, with phase angles hardly approaching -60°. This is characteristic of a significant deviation from pure capacitive behavior, thus justifying the use of constant phase element instead of conventional capacitor. The results of circuit fitting to *-Z'' vs. Z'* data of Figure 3 are provided in Table 1.

Table 1. *Results of CNLS fitting of circuit $R_s(R_{ct} Q_{dl})$ to -Z'' vs Z' data*

E / V $vs.$ Ag|AgCl	R_s / Ω cm^2	R_{ct} / kΩ cm^2	Q_{dl} / Ω^{-1} cm^{-2} s^n	n	χ^2
-0.40	55.5	8.8	0.54 10^{-4}	0.75	0.085
-0.68	52.9	6.0	0.35 10^{-4}	0.78	0.072
-1.40	54.7	2.1	0.63 10^{-4}	0.83	0.067

The calculated values of R_s and Q_{dl} are weakly dependent on electrode potential. The decrease of R_{ct} with increasing negative potential from -0.40 to -0.68 V *vs.* Ag|AgCl denotes the acceleration of the inversed reaction (3). This is not the case of the even lower value of R_{ct} at -1.4 V *vs.* Ag|AgCl because at this potential the more probable reaction is hydrogen evolution. The values of CPE exponent, n, point up to the significant deviation from the model of ideal capacitance.

The validity of $R(RQ)$ circuit suggests the occurrence of reactions with a single electron transfer step as reaction (3) and its reverse.

Within the potential range -0.1 V to 0.2 V *vs.* Ag|AgCl, where the anodic film Bi(CH$_3$O)$_{ads}$ is present, Nyquist plots obtained at various electrode potentials do not show noticeable features.

However, at these potentials Bode phase diagrams shown by the inset of Figure 4 reveal two partially overlapping time constants. This is the most clearly seen in the Bode plot measured at E = 0.15 V *vs.* Ag|AgCl, showing a deep at the frequency of 6.87 Hz.
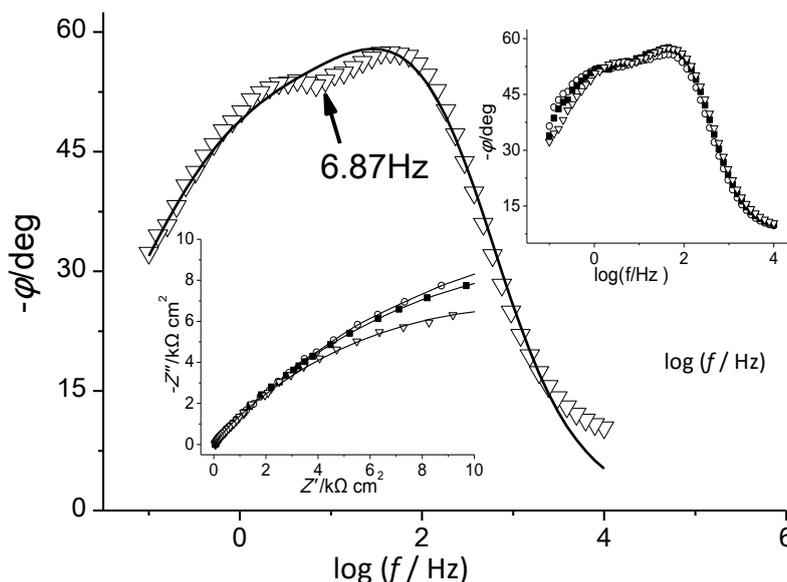
Figure 4. *Bode phase diagram of Bi in methanol solution of 0.1 M LiClO₄, at E = 0.15 V vs. Ag|AgCl. Insets: Nyquist and Bode plots at potentials ○ - 0.05, ■ - 0.10 and ▽ - 0.15 V. Lines are fitting results of R(Q[R(RQ)]) equivalent circuit to experimental points.*

Among several equivalent circuits already used for the EIS study of anodic oxides, the circuit $R_s(Q_{dl}[R_{ct}(R_{ad}\ Q_{ad})])$ shown in Figure 5, which has been suggested for the description of charge transfer process in the presence of adsorbed species [18], was applied.

The results obtained after fitting the circuit in Figure 5 to experimental impedance plots in Figure 4, are presented in Table 2.

Table 2. *Results of CNLS fitting of circuit $R_s(Q_{dl}[R_{ct}(R_{ad}\ Q_{ad})])$ to -Z'' vs. Z' data*

E / V vs. Ag|AgCl	R_s / Ω cm²	R_{ct} / kΩ cm²	Q_{dl} / Ω^{-1} cm^{-2} s^n	R_{ad} / kΩ cm²	Q_{ad} / Ω^{-1} cm^{-2} s^n	n_{dl}	n_{ad}	χ^2
-0.05	52.3	5.9	0.93 10^{-4}	28.6	0.86 10^{-4}	0.78	0.62	0.081
-0.10	52.5	7.4	0.67 10^{-4}	23.8	0.61 10^{-4}	0.890	0.75	0.088
-0.15	53.2	5.6	0.65 10^{-4}	18.9	0.49 10^{-4}	0.79	0.74	0.090
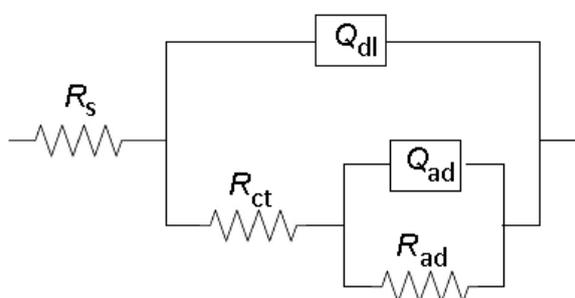
Figure 5. *Electrical equivalent circuit used to fit impedance spectrum at potentials: 0.05, 0.10 and 0.15 V vs. Ag|AgCl. R$_s$ = solution resistance, R$_{ct}$ = charge transfer resistance, R$_{ad}$= anodic film resistance. Q$_{ad}$ and Q$_{dl}$ are parameters of constant phase elements corresponding to the anodic film Bi(CH₃O)$_{ads}$ and Bi/solution interface.*

In view of the Bode plots of Figure 4 and the circuit of Figure 5, one of the two time constants may be related to the presence of Bi(CH₃O)$_{ads}$ film by means of anodic film resistance and the other to the electron transfer associated with reactions (2) and (3) by means of charge transfer resistance. The results of Table 2 reveal a high value of film resistance R_{ad} in agreement with the predicted leaky insulating character of the Bi(CH₃O)$_{ads}$ layer. As expected, R_{ct} values are lower and of similar

magnitude with those of Table 1. The values of CPE exponents, n_{dl} and n_{ad} again point up to the significant deviation of both capacitor responses from that of ideal capacitance.

Conclusions

The process of anodic film formation of bismuth in pure methanol is identified with its surface methoxylation. A single step dissolution of Bi surface to Bi^+ is suggested. Voltammetric results suggest that anodic film formation takes place within a narrow zone of low electrode potentials ranging from -0.1 V to 0.2 V *vs.* Ag|AgCl, by adsorption of $-CH_3O^-$ groups, resulting in $Bi(CH_3O)_{ads}$ film. Weak potential dependence of the out of phase *ac* current within the above potential range suggests that this film is of leaky insulating character, which is also confirmed by the relatively high value of film resistance resulting from circuit fitting to EIS measurements.

References

[1]   J. Banas, B. Stypula, K. Banas, J. Światowska-Mrowiecka, M. Starowicz, U. Lelek-Borkowska, *Journal of Solid State Electrochemistry* **13** (2009) 1669-1679.
[2]   J. Światowska-Mrowiecka, J. Banas, *Electrochimica Acta* **50** (2005) 1829-1840.
[3]   A. Papaderakis, A.G. Anastopoulos, S. Sotiropoulos, *Journal of Electroanalytical Chemistry* **783** (2016) 217-225.
[4]   J. W. Schultze, M. M. Lohrengel, *Electrochimica Acta* **45** (2000) 2499-2513 .
[5]   D. E. Williams, G. A. Wright, *Electrochimica Acta* **22** (1977) 505-508.
[6]   B. V. Tilak, R. S. Perkins, H. A. Kozlowska, B.E.Conway, *Electrochimica Acta* **17** (1972) 1447-1469.
[7]   M. Metikoš-Huković, *Electrochimica Acta* **26** (1981) 989-1000.
[8]   M. Metikoš-Huković, Z. Grubac, *The Journal of Physical Chemistry B* **102** (1998) 7406-7412.
[9]   A. Bozatzidis, A.G. Anastopoulos, T. Laopoulos, *Electroanalysis* **19** (2007) 1711-1718.
[10]   A. J. Calandra, N. R. de Tacconi, R. Pereiro, A.J. Arvia, *Electrochimica Acta* **19** (1974) 901-905.
[11]   S. Kapusta, N. Hackerman, *Electrochimica Acta* **25** (1980) 949-955.
[12]   M. Šeruga, M. Metikoš-Huković, *Journal of Electroanalytical Chemistry* **334** (1992) 223-240.
[13]   Z. Grubač, M. Metikoš-Huković, *Electrochimica Acta* **43** (1998) 3175-3181.
[14]   D. E. Williams, G. A. Wright, *Electrochimica Acta* **21** (1976) 1009-1019.
[15]   K. Lust, M. Väärtnõu, E. Lust, *Electrochimica Acta* **45** (2000) 3543-3554.
[16]   U. Stimming, J. W. Schultze, *Berichte der Bunsengesellschaft für physikalische Chemie* **80** (1976) 1297-1302.
[17]   B. A. Boukamp, *Solid State Ionics* **18-19** (1986) 136-140.
[18]   A. Lasia, *Electrochemical Impedance Spectroscopy and its Applications*, Springer, New York, USA, 2014.